

CHAPTER 6

SOLUBILITY

The treatise by Grant and Higuchi [37] comprehensively covers pre-1990 solubility literature. In this chapter, we present a concise, multimechanistic [1] solubility equilibrium model (“not just a number”; see Section 1.6) and stress what is new since 1990 [39]; we also cite some important classic works. Many protocols have been described in the literature for measuring solubility–pH profiles, using various detection systems [12,26,37–39,459–503]. Classical approaches are based on the saturation shake-flask method [37–39]. New methods are usually validated against it. The classical techniques are slow and not easily adapted to the high-throughput needs of modern drug discovery research. At the early stages of research, candidate compounds are stored as DMSO solutions, and solubility measurements need to be performed on samples introduced in DMSO, often as 10 mM solutions. It is known that even small quantities of DMSO (<5%) in water can increase the apparent solubility of molecules, and that it is a challenge to determine the true aqueous solubility of compounds when DMSO is present. To this end, a new method has been developed which extracts true aqueous solubility from DMSO-elevated values [26].

The accurate prediction of the solubility of new drug candidates still remains an elusive target [1,12,502]. Historical solubility databases used as “training sets” for prediction methods contain a large portion of oil substances, and not enough crystalline, drug-like compounds. Also, the quality of the historical data in the training sets is not always easy to verify. Such methods, for reasons of uncertain training

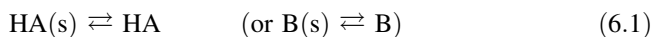
data, often perform poorly in predicting solubilities of crystalline drug compounds [504–506].

6.1 SOLUBILITY–pH PROFILES

The basic relationships between solubility and pH can be derived for any given equilibrium model. In this section simple monoprotic and diprotic molecules are considered [26,472–484,497].

6.1.1 Monoprotic Weak Acid, HA (or Base, B)

The protonation reactions for ionizable molecules have been defined in Section 3.1. When a solute molecule, HA (or B), is in equilibrium with its precipitated form, HA(s) (or B(s)), the process is denoted by the equilibrium expression



and the corresponding equilibrium constant is defined as

$$S_0 = \frac{[\text{HA}]}{[\text{HA(s)}]} = [\text{HA}] \quad \left[\text{or } S_0 = \frac{[\text{B}]}{[\text{B(s)}]} = [\text{B}] \right] \quad (6.2)$$

By convention, $[\text{HA(s)}] = [\text{B(s)}] = 1$. Eqs. (6.1) represent the precipitation equilibria of the uncharged species, and are characterized by the intrinsic solubility equilibrium constant, S_0 . The zero subscript denotes the zero charge of the precipitating species. In a saturated solution, the *effective* (total) solubility S , at a particular pH is defined as the sum of the concentrations of all the compound species dissolved in the aqueous solution:

$$S = [\text{A}^-] + [\text{HA}] \quad [\text{or } S = [\text{B}] + [\text{BH}^+]] \quad (6.3)$$

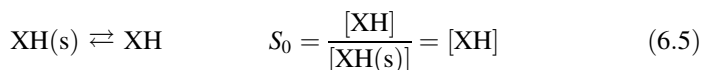
where $[\text{HA}]$ is a constant (intrinsic solubility) but $[\text{A}^-]$ is a variable. It's convenient to restate the equation in terms of only constants and with pH as the only variable. Substitution of Eqs. (3.1) [or (3.2)] into (6.3) produces the desired equation.

$$\begin{aligned} S &= \frac{[\text{HA}] K_a}{[\text{H}^+]} + [\text{HA}] && \left(\text{or } S = [\text{B}] + \frac{[\text{B}][\text{H}^+]}{K_a} \right) \\ &= [\text{HA}] \left(\frac{K_a}{[\text{H}^+]} + 1 \right) && \left(\text{or } = [\text{B}] \left\{ \frac{[\text{H}^+]}{K_a} + 1 \right\} \right) \\ &= S_0 (10^{-\text{p}K_a + \text{pH}} + 1) && \left(\text{or } = S_0 \{ 10^{+\text{p}K_a - \text{pH}} + 1 \} \right) \end{aligned} \quad (6.4)$$

Figure 6.1a shows a plot of $\log S$ versus pH for the weak-acid case (indomethacin, pK_a 4.42, $\log S_0 - 5.58$, $\log \text{mol/L } [p\text{ION}]$) and Fig. 6.2a shows that of a weak base (miconazole, pK_a 6.07, $\log S_0 - 5.85$ [$p\text{ION}$]). As is evident from the acid curve, for $\text{pH} \ll pK_a$ [i.e., $10^{-pK_a+\text{pH}} \ll 1$ in Eq. (6.4)], the function reduces to the horizontal line $\log S = \log S_0$. For $\text{pH} \gg pK_a$ (i.e., $10^{-pK_a+\text{pH}} \gg 1$), $\log S$ is a straight line as a function of pH, exhibiting a slope of +1. The base shows a slope of -1 . The pH at which the slope is half-integral equals the pK_a . Note the mirror relationship between the curve for an acid (Fig. 6.1a) and the curve for a base (Fig. 6.2a).

6.1.2 Diprotic Ampholyte, XH_2^+

In a saturated solution, the three relevant equilibria for the case of a diprotic ampholyte are Eqs. (3.3) and (3.4), plus



Note that $[\text{XH(s)}]$ by convention is defined as unity. For such a case, effective solubility is

$$S = [\text{X}^-] + [\text{XH}] + [\text{XH}_2^+] \quad (6.6)$$

where $[\text{HX}]$ is a constant (intrinsic solubility) but $[\text{X}^-]$ and $[\text{XH}_2^+]$ are variables. As before, the next step involves conversions of all variables into expressions containing only constants and pH:

$$S = S_0(1 + 10^{-pK_{a2}+\text{pH}} + 10^{+pK_{a1}-\text{pH}}) \quad (6.7)$$

Figure 6.3a shows the plot of $\log S$ versus pH of an ampholyte (ciprofloxacin, pK_a values 8.62 and 6.16, $\log S_0 - 3.72$ [$p\text{ION}$]). In Figs. 6.1b, 6.2b, and 6.3b are the log–log speciation profiles, analogous to those shown in Figs. 4.2b, 4.3b, and 4.4b. Note the discontinuities shown for the solubility speciation curves. These are the transition points between a solution containing some precipitate and a solution where the sample is completely dissolved. These log–log solubility curves are important components of the absorption model described in Section 2.1 and illustrated in Fig. 2.2.

6.1.3 Gibbs pK_a

Although Figs. 6.1a, 6.2a, and 6.3a properly convey the shapes of solubility–pH curves in saturated solutions of uncharged species, the indefinite ascendancy (dotted line) in the plots can be misleading. It is not possible to maintain saturated solutions over 10 orders of magnitude in concentration! At some point long before the solubilities reach such high values, salts will precipitate, limiting further

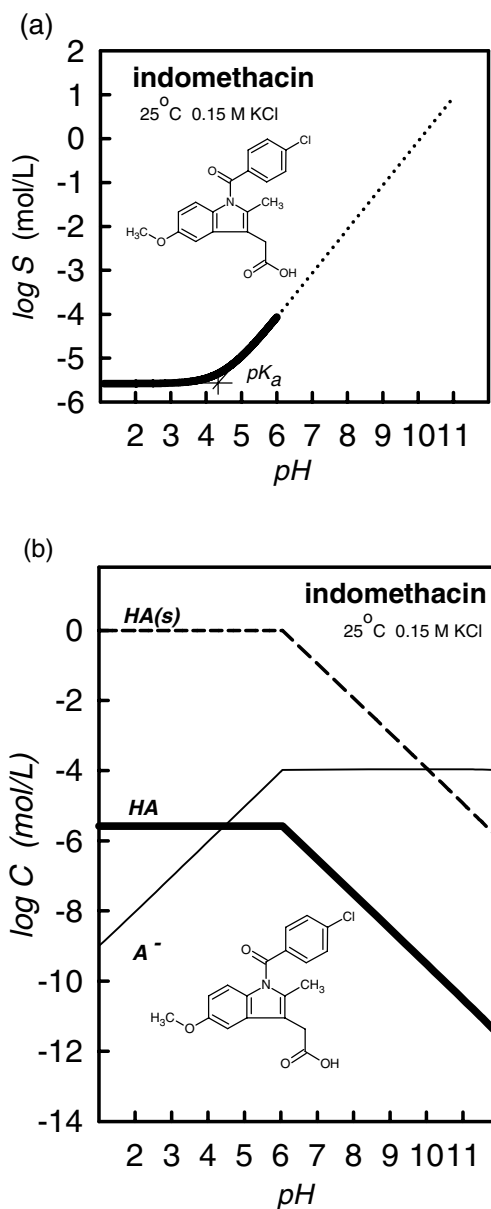


Figure 6.1 Solubility–pH profile (a) and a log–log speciation plot (b) for a weak acid (indomethacin, pK_a 4.42, $\log S_0 -5.58$ [pI_{ON}]). [Avdeef, A., *Curr. Topics Med. Chem.*, **1**, 277–351 (2001). Reproduced with permission from Bentham Science Publishers, Ltd.]

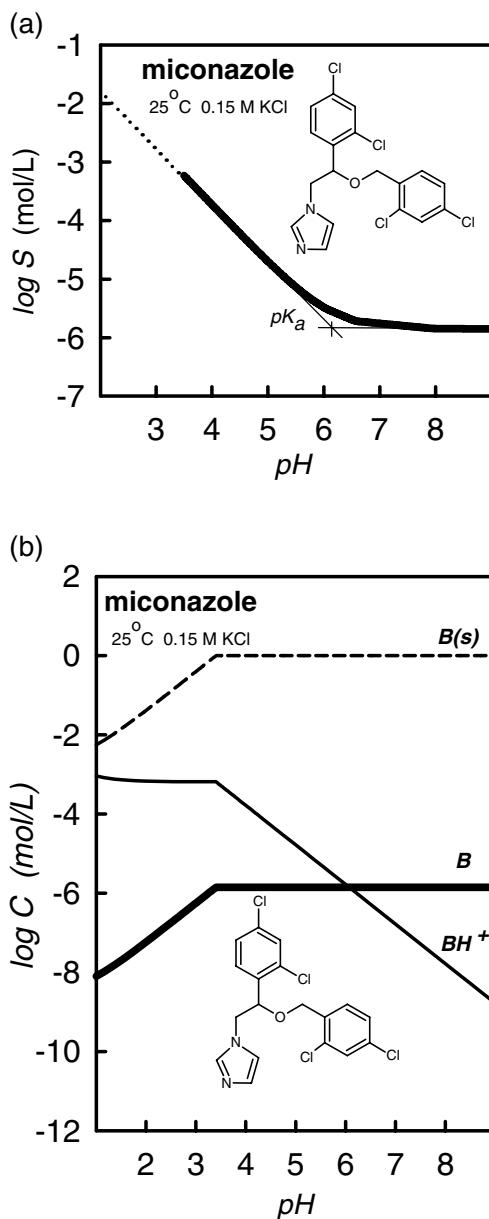


Figure 6.2 Solubility-pH profile (a) and a log-log speciation plot (b) for a weak base (miconazole, pK_a 6.07, $\log S_0 -5.85$ [pI_{ON}]). [Avdeef, A., *Curr. Topics Med. Chem.*, **1**, 277-351 (2001). Reproduced with permission from Bentham Science Publishers, Ltd.]

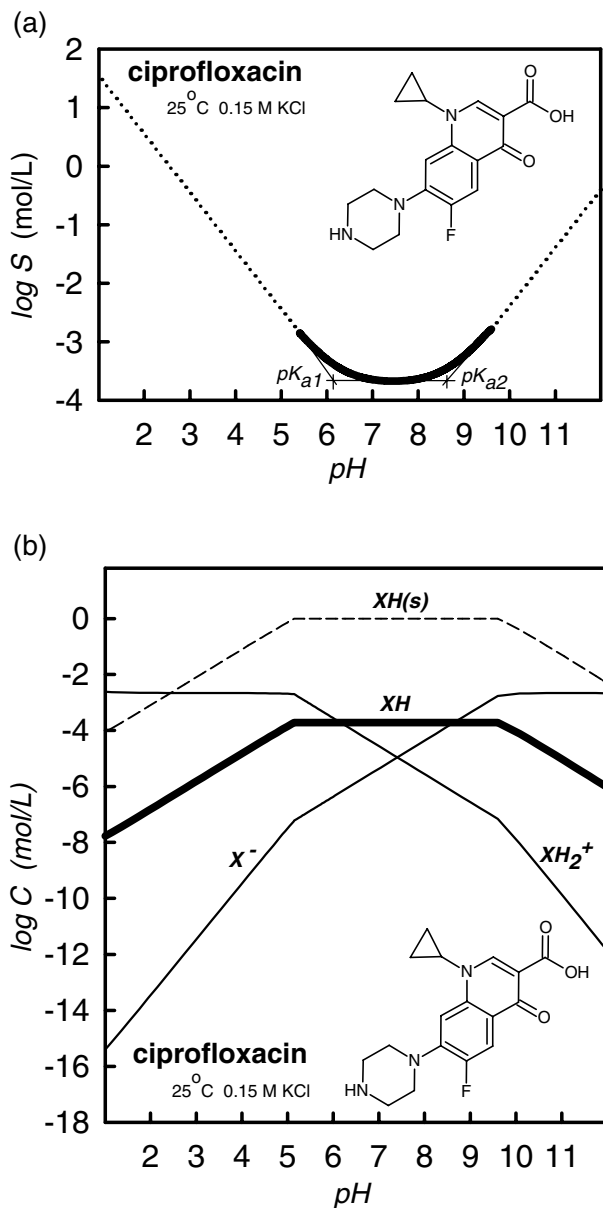


Figure 6.3 Solubility–pH profile (a) and a log–log speciation plot (b) for an ampholyte (ciprofloxacin, pK_a 8.62, 6.16, $\log S_0$ -3.72 [pION]). [Avdeef, A., *Curr. Topics Med. Chem.*, **1**, 277–351 (2001). Reproduced with permission from Bentham Science Publishers, Ltd.]

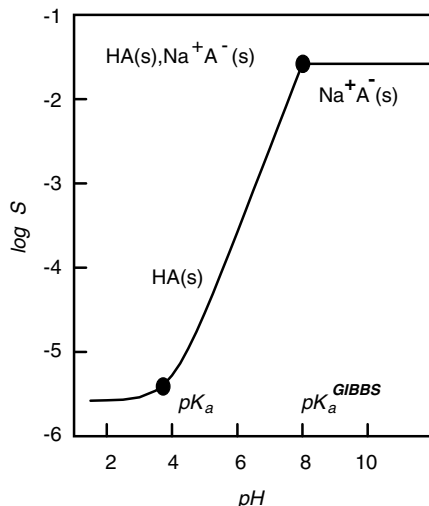
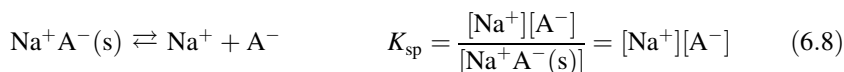


Figure 6.4 Solubility–pH profile of a weak acid, with salt precipitation taken into account. [Avdeef, A., *Curr. Topics Med. Chem.*, **1**, 277–351 (2001). Reproduced with permission from Bentham Science Publishers, Ltd.]

increases. Although precipitation of salts is not covered in detail in this chapter, it is nevertheless worthwhile to consider its formation in this limiting sense. As the pH change raises the solubility, at some value of pH the solubility product of the salt will be reached, causing the shape of the solubility–pH curve to change from that in Fig. 6.1a to that in Fig. 6.4, an example of a weak acid exhibiting salt precipitation.

As a new rule of thumb [473], in 0.15 M NaCl (or KCl) solutions titrated with NaOH (or KOH), acids start to precipitate as salts above $\log (S/S_0) \approx 4$ and bases above $\log (S/S_0) \approx 3$. It is exactly analogous to the *diff* 3–4 rule; let us call the solubility equivalent the “*sdiff* 3–4” rule [473]. Consider the case of the monoprotic acid HA, which forms the sodium salt (in saline solutions) when the solubility product K_{sp} is exceeded. In addition to Eqs. (3.1) and (6.1), one needs to add the following reaction/equation to treat the case:



Effective solubility is still defined by Eq. (6.3). However, Eq. (6.3) is now solved under three limiting conditions with reference to a special pH value:

1. If the solution pH is below the conditions leading to salt formation, the solubility–pH curve has the shape described by Eq. (6.4) (curve in Fig. 6.1a).
2. If pH is above the characteristic value where salt starts to form (given high enough a sample concentration), Eq. (6.3) is solved differently. Under

this circumstance, $[A^-]$ becomes the constant term and $[HA]$ becomes variable.

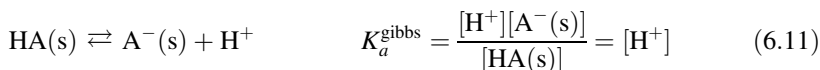
$$\begin{aligned}
 S &= [A^-] + \frac{[H^+][A^-]}{K_a} \\
 &= [A^-] \left(1 + \frac{[H^+]}{K_a} \right) \\
 &= \frac{K_{sp}}{[Na^+]} (1 + 10^{+pK_a - pH}) \\
 &= S_i (1 + 10^{+pK_a - pH}) \tag{6.9}
 \end{aligned}$$

where S_i refers to the solubility of the conjugate base of the acid, which depends on the value of $[Na^+]$ and is hence a conditional constant. Since $pH \gg pK_a$ and $[Na^+]$ may be assumed to be constant, Eq. (6.9) reduces to that of a horizontal line in Fig. 6.4: $\log S = \log S_i$ for $pH > 8$.

3. If the pH is exactly at the special point marking the onset of salt precipitation, the equation describing the solubility-pH relationship may be obtained by recognizing that both terms in Eq. 6.3 become constant, so that

$$S = S_0 + S_i \tag{6.10}$$

Consider the case of a very concentrated solution of the acid hypothetically titrated from low pH ($< pK_a$) to the point where the solubility product is first reached (high pH). At the start, the saturated solution can only have the uncharged species precipitated. As pH is raised past the pK_a , the solubility increases, as more of the free acid ionizes and some of the solid HA dissolves, as indicated by the solid curve in Fig. 6.1a. When the solubility reaches the solubility product, at a particular elevated pH, salt starts to precipitate, but at the same time there may be remaining free acid precipitate. The simultaneous presence of the solid free acid and its solid conjugate base invokes the Gibbs phase rule constraint, forcing the pH and the solubility to constancy, as long as the two interconverting solids are present. In the course of the thought-experiment titration, the alkali titrant is used to convert the remaining free acid solid into the solid salt of the conjugate base. During this process, pH is absolutely constant (a “perfect” buffer system). This special pH point has been designated the Gibbs pK_a , that is, pK_a^{gibbs} [472,473]. The equilibrium equation associated with this phenomenon is



Note that pK_a^{gibbs} is the conceptual equivalent of pK_a^{oct} and pK_a^{mem} [(see. Eq. (5.1)]. We should not be surprised that this is a *conditional* constant, depending on the value of the background salt.

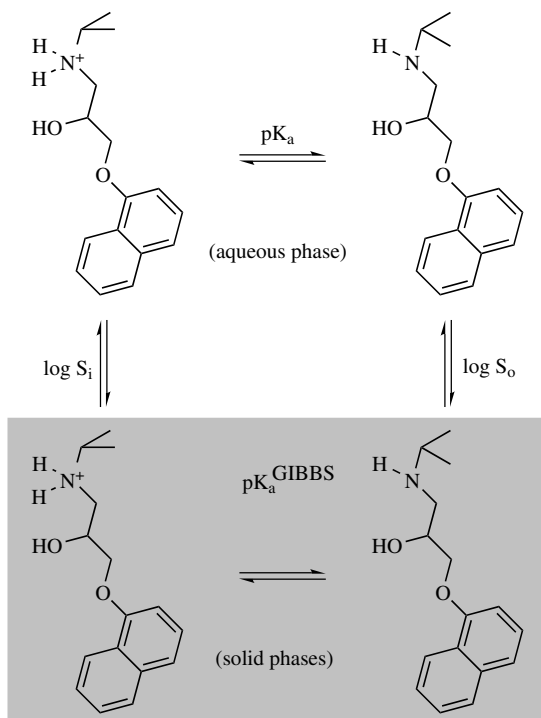


Figure 6.5 Solubility tetrad equilibria. [Avdeef, A., *Curr. Topics Med. Chem.*, **1**, 277–351 (2001). Reproduced with permission from Bentham Science Publishers, Ltd.]

At this point we bring in the now familiar tetrad diagram, Fig. 6.5, and conclude that

$$sdiff(\log S^{I-N}) = \log S_i - \log S_o = |pK_a^{\text{gibbs}} - pK_a| \quad (6.12)$$

Figure 6.4 shows a hypothetical solubility–pH profile with $sdiff = 4$, as typical as one finds with simple acids in the presence of 0.15 M Na^+ or K^+ [473]. Compare Eq. (6.12) with Eq. (4.6).

In principle, all the curves in Figs. 6.1a, 6.2a, and 6.3a would be expected to have solubility limits imposed by the salt formation. Under conditions of a constant counterion concentration, the effect would be indicated as a point of discontinuity (pK_a^{gibbs}), followed by a horizontal line of constant solubility S_i .

6.2 COMPLICATIONS MAY THWART RELIABLE MEASUREMENT OF AQUEOUS SOLUBILITY

There are numerous experimental complications in the measurement of solubility. Solid phases, formed incipiently, are often metastable with respect to a

thermodynamically more stable phase, especially with highly insoluble compounds. An “active” form of a solid, a very fine crystalline precipitate with a disordered lattice, can drop out of a strongly oversaturated solution, which then “ages” only slowly into a more stable “inactive” form [465]. Hence, if measurements are done following initial precipitation, higher solubilities are observed. Amorphism [464] and polymorphism [466] can be troubling complications. Various solvates of a solid (either water or cosolvent in the crystal lattice) have different solubilities [43].

Certain surface-active compounds [499], when dissolved in water under conditions of saturation, form self-associated aggregates [39,486–488] or micelles [39,485], which can interfere with the determination of the true aqueous solubility and the pK_a of the compound. When the compounds are very sparingly soluble in water, additives can be used to enhance the rate of dissolution [494,495]. One can consider DMSO used in this sense. However, the presence of these solvents can in some cases interfere with the determination of the true aqueous solubility. If measurements are done in the presence of simple surfactants [500], bile salts [501], complexing agents such as cyclodextrins [489–491,493], or ion-pair-forming counterions [492], extensive considerations need to be applied in attempting to extract the true aqueous solubility from the data. Such corrective measures are described below.

6.3 DATABASES AND THE “IONIZABLE MOLECULE PROBLEM”

Two sensibly priced commercial databases for solubility exist [366,507]. An article in the journal *Analytical Profiles of Drug Substances* carries solubility data [496]. Abraham and Le [508] published a list of intrinsic aqueous solubilities of 665 compounds, with many ionizable molecules. It is difficult to tell from published lists what the quality of the data for *ionizable* molecules is. Sometimes, it is not clear what the listed number stands for. For example, S_w , water solubility, can mean several different things: either intrinsic value, or value determined at a particular pH (using buffers), or value measured by saturating distilled water with excess compound. In the most critical applications using ionizable molecules, it may be necessary to scour the original publications in order to be confident of the quality of reported values.

6.4 EXPERIMENTAL METHODS

Lipinski et al. [12] and Pan et al. [463] compared several commonly used methods of solubility measurement in early discovery, where samples are often introduced as 10 mM DMSO solutions. Turbidity-based and UV plate scanner-based detections systems were found to be useful. The methods most often used in discovery and in preformulation will be briefly summarized below.

6.4.1 Saturation Shake-Flask Methods

Solubility measurement at a single pH [37–39] under equilibrium conditions is largely a labor-intensive procedure, requiring long equilibration times (12 h–7 days). It's a simple procedure. The drug is added to a standard buffer solution (in a flask) until saturation occurs, indicated by undissolved excess drug. The thermostated saturated solution is shaken as equilibration between the two phases is established. After microfiltration or centrifugation, the concentration of the substance in the supernatant solution is then determined using HPLC, usually with UV detection. If a solubility–pH profile is required, then the measurement needs to be performed in parallel in several different pH buffers.

6.4.2 Turbidimetric Ranking Assays

Turbidity-detection-based methods [12,459–463], popularized by Lipinski and others, in part have met some high-throughput needs of drug discovery research. The approach, although not thermodynamically rigorous, is an attempt to rank molecules according to expected solubilities. Usually, the measurements are done at one pH. Various implementations of the basic method are practiced at several pharmaceutical companies, using custom-built equipment. Detection systems based on 96-well microtiter plate nephelometers are well established. An automated solubility analyzer incorporating such a detector usually requires the user to develop an appropriate chemistry procedure and to integrate a robotic fluidic system in a customized way. It is important that turbidity methods using an analate addition strategy be designed to keep the DMSO concentration in the buffer solution constant in the course of the additions. The shortcomings of the turbidity methodology are (1) poor reproducibility for very sparingly water-soluble compounds, (2) use of excessive amounts ($\leq 5\%$ v/v) of DMSO in the analate addition step, and (3) lack of standardization of practice.

6.4.3 HPLC-Based Assays

In an effort to increase throughput, several pharmaceutical companies have transferred the classical saturation shake-flask method to 96-well plate technology using a robotic liquid dispensing system [463]. Analyses are performed with fast generic gradient reverse-phase HPLC. In some companies, the DMSO is eliminated by a freeze-drying procedure before aqueous buffers are added. This adds to the assay time and can be problematic with volatile samples (e.g., coumarin). Still, the serial chromatographic detection systems are inherently slow. Data handling and report generation are often the rate-limiting steps in the operations.

6.4.4 Potentiometric Methods

Potentiometric methods for solubility measurement have been reported in the literature [467–471]. A novel approach, called *dissolution template titration* (DTT), has been introduced [472–474]. One publication called it the “gold standard” [509].

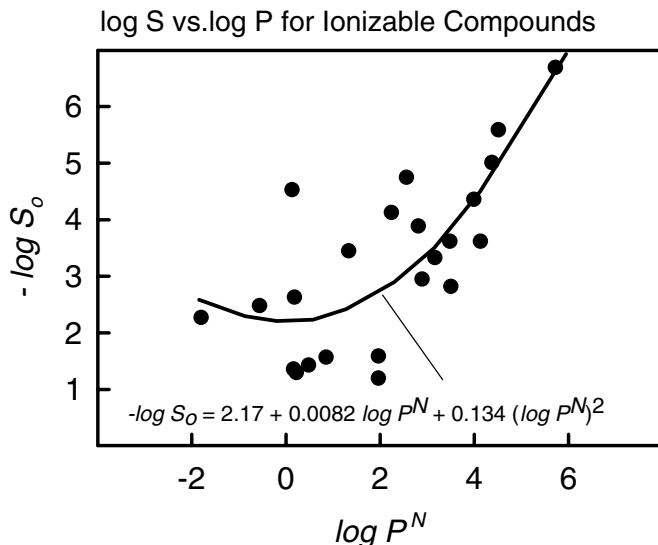


Figure 6.6 Empirical relationship between intrinsic solubility of ionizable molecules and their octanol–water log P [pION]. [Avdeef, A., *Curr. Topics Med. Chem.*, **1**, 277–351 (2001). Reproduced with permission from Bentham Science Publishers, Ltd.]

The procedure takes as input parameters the measured (or calculated) pK_a and the measured (or calculated) octanol–water partition coefficient, $\log P$. The latter parameter is used to estimate the intrinsic solubility S_0 , using the Hansch-type expression [38], $\log S_0 = 1.17 - 1.38 \log P$, or an improved version for ionizable molecules of moderate lipophilicity (Fig. 6.6):

$$\log S_0 = -2.17 - 0.0082 \log P - 0.134(\log P)^2 \quad (6.13)$$

Using the pK_a and the estimated S_0 , the DTT procedure simulates the entire titration curve before the assay commences. Figure 6.7 shows such a titration curve of propoxyphene. The simulated curve serves as a template for the instrument to collect individual pH measurements in the course of the titration. The pH domain containing precipitation is apparent from the simulation (filled points in Fig. 6.7). Titration of the sample suspension is done in the direction of dissolution (high to low pH in Fig. 6.7), eventually well past the point of complete dissolution ($\text{pH} < 7.3$ in Fig. 6.7). The rate of dissolution of the solid, described by the classical Noyes–Whitney expression [37], depends on a number of factors, which the instrument takes into account. For example, the instrument slows down the rate of pH data taking as the point of complete dissolution approaches, where the time needed to dissolve additional solid substantially increases (between pH 9 and 7.3 in Fig. 6.7). Only after the precipitate completely dissolves, does the instrument collect the remainder of the data rapidly (unfilled circles in Fig. 6.7). Typically, 3–10 h is required for the entire equilibrium solubility data taking. The more insoluble the

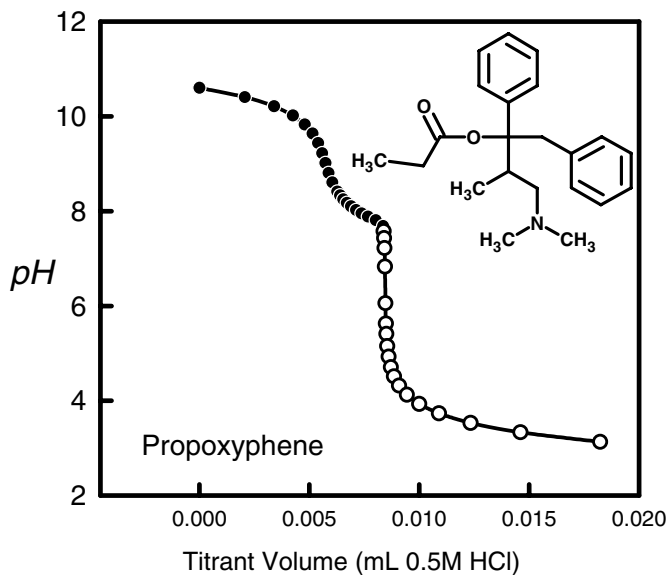


Figure 6.7 Dissolution template titration (DTT) curve of propoxyphene: 0.51 mg of the hydrochloride salt was dissolved in 5.1 mL of 0.15 M KCl solution, with 0.0084 mL of 0.5 M KOH used to raise the pH to 10.5.

compound is anticipated to be (based on the template) the longer the assay time. An entire solubility–pH profile is deduced from the assay.

A graphical analysis follows, based on Bjerrum plots (see Sections 3.3.1 and 4.14). The Bjerrum difference plots are probably the most important graphical tools in the initial stages of solution equilibrium analysis in the pH-metric method. The difference curve is a plot of \bar{n}_H , the average number of bound protons (i.e., the hydrogen ion binding capacity), versus p_cH ($-\log [H^+]$). Such a plot can be obtained by subtracting a titration curve containing no sample (“blank” titration) from a titration curve with sample; hence the term “difference” curve. Another way of looking at it is as follows. Since it is known how much strong acid [HCl] and strong base [KOH] have been added to the solution at any point and since, it is known how many dissociable protons n the sample substance brings to the solution, the *total* hydrogen ion concentration in solution is known, regardless of what equilibrium reactions are taking place (model independence). By measuring the pH, and after converting it into p_cH [116], the *free* hydrogen ion concentration is known. The difference between the total and the free concentrations is equal to the concentration of the *bound* hydrogen ions. The latter concentration divided by that of the sample substance C gives the average number of bound hydrogen ions per molecule of substance \bar{n}_H

$$\bar{n}_H = \frac{([HCl] - [KOH] + nC - [H^+] + K_w/[H^+])}{C} \quad (6.14)$$

where K_w is the ionization constant of water (1.78×10^{-14} at 25°C, 0.15 M ionic strength).

Figure 6.8 shows the Bjerrum plots for a weak acid (benzoic acid, pK_a 3.98, $\log S_0 - 1.55$, $\log \text{mol/L}$ [474]), a weak base (benzylamine, pK_a 9.26, $\log S_0 - 3.83$, $\log \text{mol/L}$ [472]), and an ampholyte (acyclovir, pK_a 2.34 and 9.23, $\log S_0 - 2.16$, $\log \text{mol/L}$ [p ION]). These plots reveal the pK_a and pK_a^{app} values as the $p_c\text{H}$ values at half-integral \bar{n}_H positions. By simple inspection of the dashed curves in Fig. 6.8, the pK_a values of the benzoic acid, benzylamine, and acyclovir are 4.0, 9.3, and (2.3, 9.2), respectively. The pK_a^{app} values depend on the concentrations used, as is evident in Fig. 6.8. It would not have been possible to deduce the constants by simple inspection of the titration curves (pH vs. volume of titrant, as in Fig. 6.7). The difference between pK_a and pK_a^{app} can be used to determine $\log S_0$, the intrinsic solubility, or $\log K_{\text{sp}}$, the solubility product of the salt, as will be shown below.

In addition to revealing constants, Bjerrum curves are a valuable diagnostic tool that can indicate the presence of chemical impurities and electrode performance problems [165]. Difference curve analysis often provides the needed “seed” values for refinement of equilibrium constants by mass-balance-based nonlinear least squares [118].

As can be seen in Fig. 6.8, the presence of precipitate causes the apparent pK_a , pK_a^{app} , to shift to higher values for acids and to lower values for bases, and in opposite but equal directions for ampholytes, just as with octanol (Chapter 4) and liposomes (Chapter 5). The intrinsic solubility can be deduced by inspection of the curves and applying the relationship [472]

$$\log S_0 = \log \frac{C}{2} - |pK_a^{\text{app}} - pK_a| \quad (6.15)$$

where C is the sample concentration. To simplify Eq. (6.15), Fig. 6.9 shows characteristic Bjerrum plots taken at 2 M concentration of an acid (ketoprofen, $\log S_0 - 3.33$ [473]), a base (propranolol, $\log S_0 - 3.62$ [473]), and an ampholyte (enalapril maleate, $\log S_0 - 1.36$ [474]). In Fig. 6.9, all examples are illustrated with $C = 2\text{ M}$, so that the difference between true pK_a and the apparent pK_a is directly read off as the $\log S_0$ value.

In an ideally designed experiment, only a *single* titration is needed to determine the solubility constant *and* the aqueous pK_a . This is possible when the amount of sample, such as a weak base, added to solution is such that from the start of an alkalimetric titration ($\text{pH} \ll pK_a$) to the midbuffer region ($\text{pH} = pK_a$) the compound stays in solution, but from that point to the end of titration ($\text{pH} \gg pK_a$), precipitation occurs. (The idea is similar to that described by Seiler [250] for $\log P$ determinations by titration.) After each titrant addition, pH is measured. The curve represented by unfilled circles in Fig. 6.8b is an example of such a titration of a weak base whose pK_a is 9.3, with precipitation occurring above pH 9.3, with onset indicated by the “kink” in the curve at that pH. In practice, it is difficult to know *a priori* how much compound to use in order to effect such a special condition. So, two or more titrations may be required, covering a probable range of concentrations,

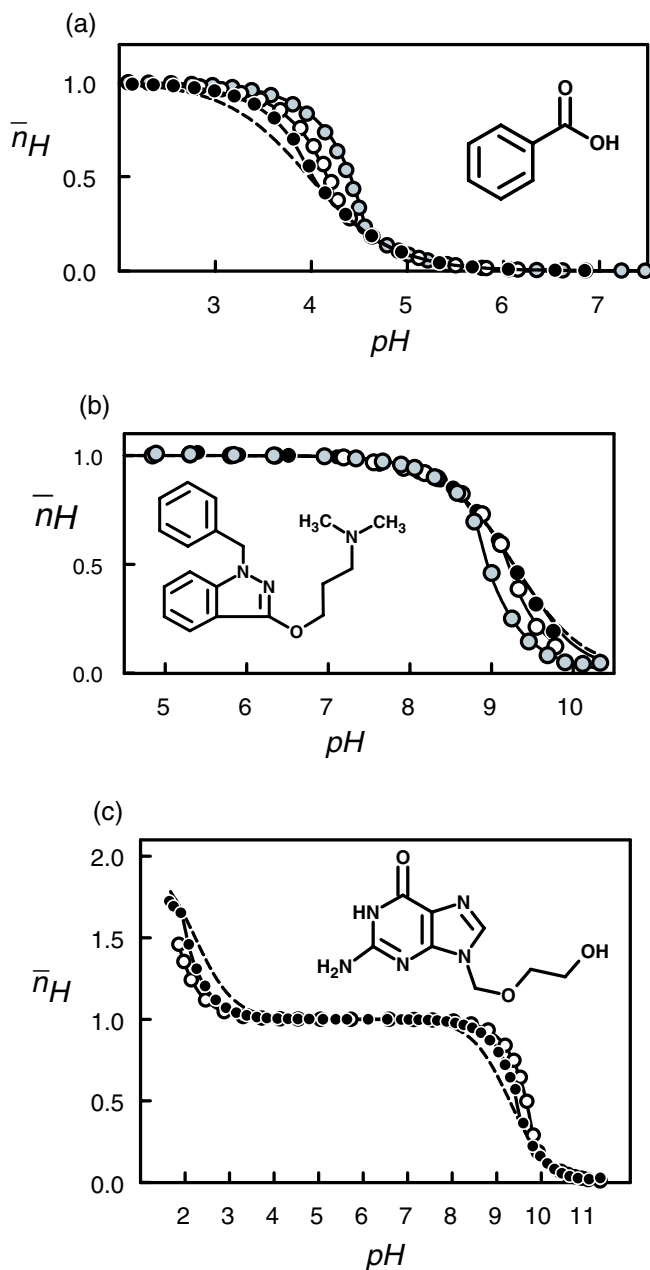


Figure 6.8 Bjerrum plots for (a) benzoic acid (black circle = 87 mM, unfilled circle = 130 mM, gray circle = 502 mM), (b) benzydamine (black circle = 0.27 mM, unfilled circle = 0.41 mM, gray circle = 0.70 mM), and (c) acyclovir (black circle = 29 mM, unfilled circle = 46 mM). The dashed curves correspond to conditions under which no precipitation takes place.

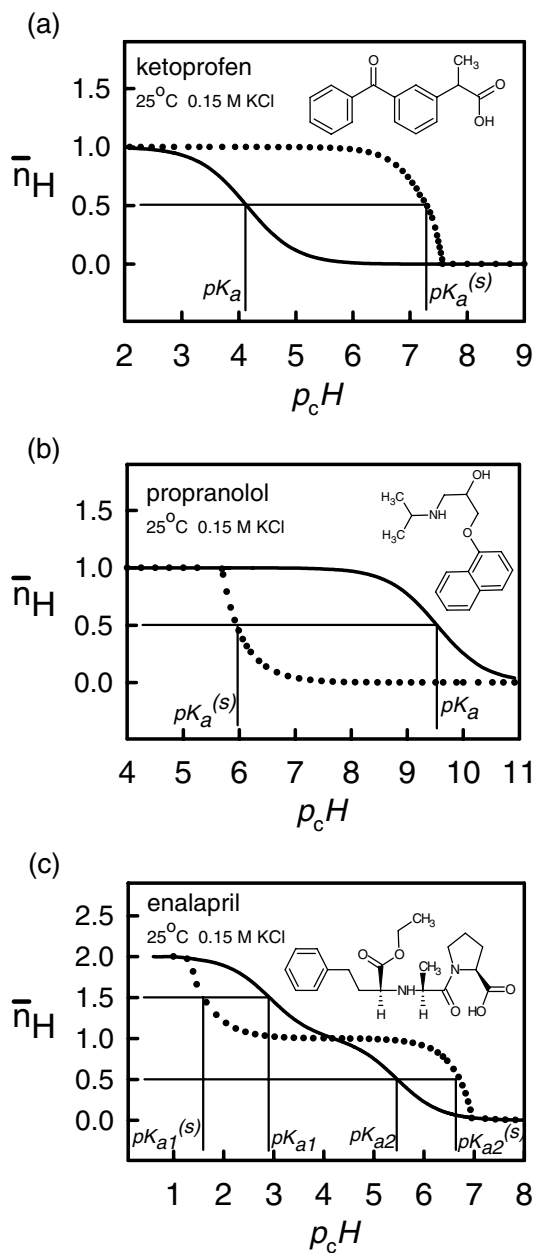


Figure 6.9 Simulated Bjerrum plots of saturated solutions of an acid, a base, and an ampholyte. The sample concentration was chosen as 2 M, a special condition where the difference between the true pK_a and the apparent pK_a is equal to $-\log S_0$. [Avdeef, A., *Curr. Topics Med. Chem.*, **1**, 277–351 (2001). Reproduced with permission from Bentham Science Publishers, Ltd.]

using as little sample as necessary to cause precipitation near the mid-point. For compounds extremely insoluble in water, cosolvents such as methanol, ethanol, DMSO, or acetonitrile may be used, with the solubility constant determined by extrapolation to zero cosolvent [43].

Usually, the solubility of the salt is determined from separate, more concentrated solutions. To conserve on sample, the titration of the salt may be performed with an excess of the counterion concentration [479]. Also, some amount of sample salt may be conserved by titrating in cosolvent mixtures, where salts are often less soluble.

The graphically deduced constants are subsequently refined by a weighted non-linear least squares procedure [472]. Although the potentiometric method can be used in discovery settings to calibrate high-throughput solubility methods and computational procedures, it is too slow for HTS applications. It is more at home in a preformulation lab.

6.4.5 Fast UV Plate Spectrophotometer Method

A high-throughput method using a 96-well microtiter plate format and plate UV spectrophotometry has been described [26]. Solubilities at a single pH, or at ≤ 12 pH values can be determined, using one of two methods.

6.4.5.1 Aqueous Dilution Method

A known quantity of sample is added to a known volume of a universal buffer solution of sufficient capacity and of known pH. The amount of sample must be sufficient to cause precipitation to occur in the formed saturated solution. After waiting for a period of time to allow the saturated solution to reach the desired steady state, the solution is filtered to remove the solid and obtain a clear solution, whose spectrum is then taken by the UV spectrophotometer. Mathematical treatment of the spectral data yields the area-under-the-curve of the filtered sample solution, AUC_S .

A reference solution is prepared by a dilution method. A known quantity of sample is dissolved in a known volume of the system buffer of known pH; the amount of sample is X times less than in the above case in order to avoid precipitation in the formed solution. The spectrum is immediately taken by the UV spectrophotometer, to take advantage of the possibility that solution may be “supersaturated” (i.e., solid should have precipitated, but because not enough time was allowed for the solid to precipitate, the solution was temporarily clear and free of solid). Mathematical treatment of the spectral data yields the AUC of the reference sample solution, AUC_R . The ratio $R = AUC_R/AUC_S$ is used to automatically recognize the right conditions for solubility determination: when the reference has no precipitate, and the sample solution is saturated with precipitate. Under these conditions, solubility is determined from the expression

$$S = \frac{C_R}{R} \quad (6.16)$$

TABLE 6.1 Intrinsic Solubility S_0 , Corrected for the Drug DMSO/Drug Aggregation Effects

Compound	pK_a	S_0^{APP} ($\mu\text{g/mL}$)	Corrected S_0 ($\mu\text{g/mL}$)	pSOL S_0 ($\mu\text{g/mL}$)	Shake-Flask S_0 ($\mu\text{g/mL}$)
Amitriptyline	9.45 ^a	56.9	3.0	2.0 ^a	2.0 ^a
Chlorpromazine	9.24 ^a	19.4	3.4	3.5 ^a	0.1 ^a
Diclofenac	3.99 ^b	22.6	3.8	0.8 ^b	0.6 ^b
Furosemide	10.63, 3.52 ^b	29.8	2.9	5.9 ^b	12.0 ^b (2.9 ^c)
Griseofulvin	Nonionizable	37.6	20.2	—	9 ^d
Indomethacin	4.42 ^a	7.2	4.1	2.0 ^a	2.0 ^a , 1 ^e
Miconazole	6.07 ^f	11.1	1.6	0.7 ^f	—
2-Naphthoic acid	4.16 ^f	33.3	20.2	—	22.4 ^g
Phenazopyridine	5.15 ^f	12.2	12.2	14.3 ^f	—
Piroxicam	5.07, 2.33 ^h	10.5	1.1	—	9.1 ⁱ (3.3 ^c), 8–16 ^j (2.2–4.4 ^c)
Probenecid	3.01 ^f	4.6	0.7	0.6 ^f	—
Terfenadine	9.53 ^f	4.4	0.1	0.1 ^f	—

^aM. A. Strafford, A. Avdeef, P. Artursson, C. A. S. Johansson, K. Luthman, C. R. Brownell, and R. Lyon, Am. Assoc. Pharm. Sci. Ann. Mtng. 2000, poster presentation.

^bRef. 433.

^cCorrected for aggregate formation: unpublished data.

^dJ. Huskonen, M. Salo, and J. Taskinen, *J. Chem. Int. Comp. Soc.* **38**, 450–456 (1998).

^eRef. 507.

^fpION, unpublished data.

^gK. G. Mooney, M. A. Mintun, K. J. Himmestein, and V. J. Stella, *J. Pharm. Sci.* **70**, 13–22 (1981).

^hRef. 162.

ⁱC. R. Brownell, FDA, private correspondence, 2000.

^jRef. 500 (24 h).

where C_R is the calculated concentration of the reference solution. Some results are presented in Table 6.1. The apparent intrinsic solubilities S_0^{app} , determined in this way (eq. 6.16) are listed in column 3, for the compounds used in one study. All the S_0^{app} values reported in Table 6.1 were determined in the presence of 0.5% v/v DMSO, except for phenazopyridine, where 0.26% was used.

The results of a pH 4–9.5 solubility assay of chlorpromazine are shown in Fig. 6.10. The horizontal line represents the upper limit of measurable solubility (e.g., 125 $\mu\text{g/mL}$), which can be set by the instrument according to the requirements of the assay. When the measured concentration reaches the line, the sample is completely dissolved, and solubility cannot be determined. This is automatically determined by the instrument, based on the calculated value of R . When measured points fall below the line, the concentration corresponds to the apparent solubility S^{app} .

6.4.5.2 Cosolvent Method

The sample plate is prepared as in the preceding method. But before the spectra are taken, a volume Y of a water-miscible cosolvent is added to a volume Z of sample

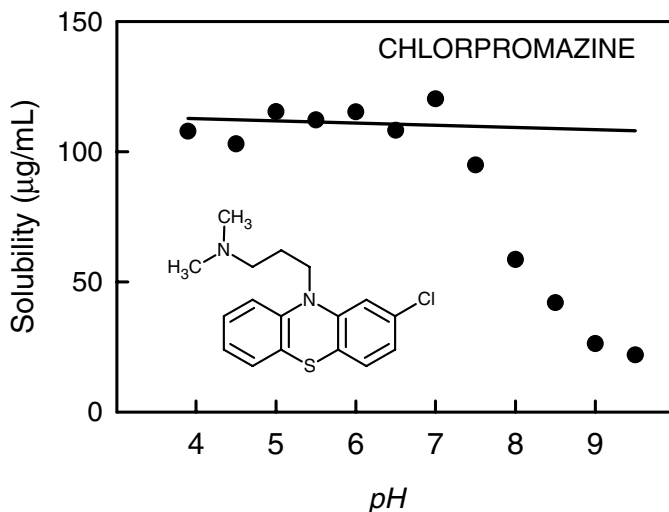


Figure 6.10 High-throughput solubility–pH determination of chlorpromazine. The horizontal line indicates the set upper limit of solubility, where the compound completely dissolves and solubility cannot be specified. The points below the horizontal line are measured in the presence of precipitation and indicate solubility. The solubility–pH curve was collected in the presence of 0.5 vol% DMSO, and is affected by the cosolvent (see text). [Avdeef, A., *Curr. Topics Med. Chem.*, **1**, 277–351 (2001). Reproduced with permission from Bentham Science Publishers, Ltd.]

solution to produce a new solution, in which the compound is now diluted by $Z/(Y + Z)$. Suitable cosolvents are ones with the lowest vapor pressure, the greatest capability in dissolving a solute (i.e., highest solubilizing power) and the lowest UV absorption. The spectrum of the solution is then immediately taken by the UV spectrophotometer. Mathematical treatment of the spectral data yields the area under the curve of the filtered cosolvent sample solution, AUC_S^{COS} .

The reference plate is prepared differently. A known quantity of sample is added to a known volume of system solution of known pH with the amount of sample *comparable* to that found in the sample plate, and no effort is made in this step to suppress precipitation in the formed solution. A volume Y of the cosolvent is immediately added to a volume Z of reference solution to produce a new solution, in which the compound is now diluted by $Z/(Y + Z)$. The spectrum of the solution is then immediately taken by the UV spectrophotometer. Mathematical treatment of the spectral data yields the area under the curve of the cosolvent reference solution, AUC_R^{COS} . Define $R^{\text{COS}} = AUC_R^{\text{COS}}/AUC_S^{\text{COS}}$. The solubility of the sample compound then is

$$S = \frac{(1 + Y/Z)C_R^{\text{COS}}}{R^{\text{COS}}} \quad (6.17)$$

where C_R^{COS} is the calculated concentration of the compound in the reference solution.

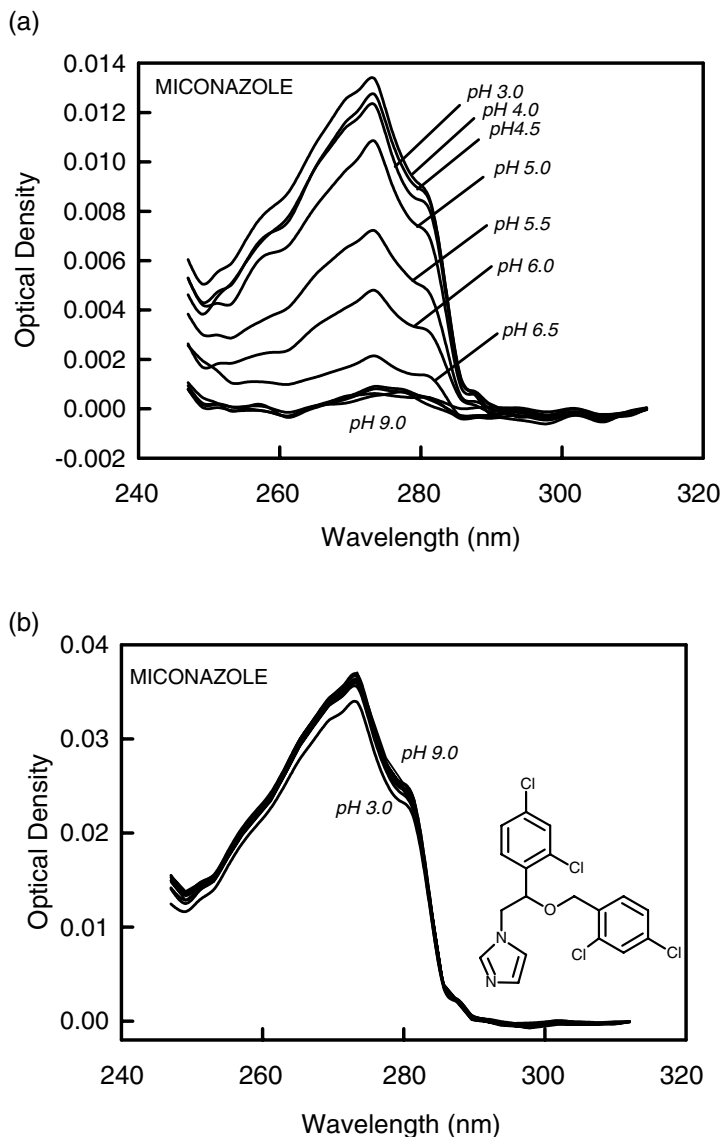


Figure 6.11 UV spectra of saturated solutions of miconazole as a function of pH: (a) sample; (b) reference. [Avdeef, A., *Curr. Topics Med. Chem.*, **1**, 277–351 (2001). Reproduced with permission from Bentham Science Publishers, Ltd.]

Figure 6.11 shows the measured absorption spectra of miconazole (reference and sample). As precipitation takes place to varying degrees at different pH values, the spectra of the sample solutions change in optical densities, according to Beer's law. This can be clearly seen in Fig. 6.12 for the sample spectra, where the sample spectra have the lowest OD values at pH 9.0 and systematically show higher OD values

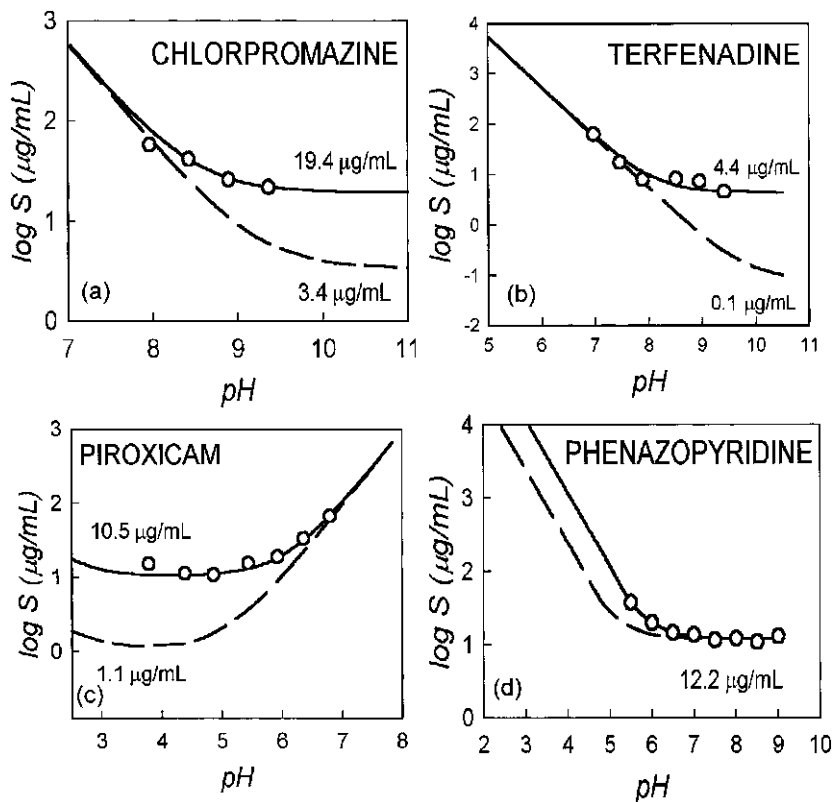


Figure 6.12 Correction of the apparent solubility–pH profile (solid curves) for the effect of DMSO and/or aggregation: (a) chlorpromazine; (b) terfenadine; (c) piroxicam; (d) phenazopyridine. [Avdeef, A., *Curr. Topics Med. Chem.*, **1**, 277–351 (2001). Reproduced with permission from Bentham Science Publishers, Ltd.]

as pH is lowered, a pattern consistent with that of a weak base. The changing OD values indicate that solubility changes with pH.

6.5 CORRECTION FOR THE DMSO EFFECT BY THE Δ -SHIFT METHOD

6.5.1 DMSO Binding to the Uncharged Form of a Compound

It was found that the $\log S/\text{pH}$ curves were altered in the presence of as little as 0.5% v/v DMSO, in that the apparent $\text{p}K_a$ values, $\text{p}K_a^{\text{app}}$, derived from $\log S$ versus pH [481], were different from the true $\text{p}K_a$ values by about one log unit. The $\text{p}K_a^{\text{app}}$ values were generally higher than the true $\text{p}K_a$ values for weak acids (positive shift), and lower than those for weak bases (negative shift). This has been called

the “ Δ shift” [Avdeef, unpublished]. It is thought to be caused in some cases by DMSO binding to the drugs. Just as the equilibrium model in Section 6.1.3 was expanded to allow for the salt solubility equilibrium, Eq. (6.4), the same can be done with a binding equation based on DMSO (e.g., in 0.5% v/v);



Such a reaction can cause a shift in the apparent ionization constant. It was discovered that the Δ shift, when subtracted from the logarithm of the apparent (DMSO-distorted) solubility S_0^{APP} , yields the true aqueous solubility constant:

$$\log S_0 = \log S_0^{\text{APP}} \pm \Delta \quad (6.19)$$

where \pm includes $-$ for acids and $+$ for bases. For an amphoteric molecule (which has both acid and base functionality) with two $\text{p}K_a$ values either sign may be used, depending on which of the two values is selected. DMSO makes the compound appear more soluble, but the true aqueous solubility can be determined from the apparent solubility by subtracting the $\text{p}K_a$ difference. Figure 6.12 illustrates the apparent solubility–pH curve (solid line) and the true aqueous solubility–pH curve (dashed line), correcting for the effect of DMSO for several of the molecules considered.

6.5.2 Uncharged Forms of Compound–Compound Aggregation

Shifts in $\text{p}K_a$ can also be expected if water-soluble aggregates form from the uncharged monomers. This may be expected with surface-active molecules or molecules such as piroxicam [500]. Consider the case where no DMSO is present, but aggregates form, of the sort



The working assumption is that the aggregates are water soluble, that they effectively make the compound appear more soluble. If ignored, they will lead to erroneous assessment of intrinsic solubility. It can be shown that Eq. (6.19) also applies to the case of aggregation.

6.5.3 Compound–Compound Aggregation of Charged Weak Bases

Consider the case of a weak base, where the *protonated*, positively charged form self-associates to form aggregates, but the uncharged form does not. This may be the case with phenazopyridine (Fig. 6.12). Phenazopyridine is a base that consistently shows *positive* shifts in its apparent $\text{p}K_a$, the opposite of what’s expected

of uncharged compound DMSO or aggregation effects. A rationalization of this effect can be based on the formation of partially protonated aggregates (perhaps micelles). Assume that one of the species is $(\text{BH}^+)_n$.



It can be shown that for such a case, the observed solubility–pH curve is shifted horizontally, not vertically, as with uncharged-compound DMSO/aggregation effects, and that the apparent intrinsic solubility is not affected by the phenomenon.

6.5.4 Ionizable Compound Binding by Nonionizable Excipients

It can be postulated that a number of phenomena, similar to those of reactions in Eqs. (6.17), (6.19), and (6.20), will shift the apparent $\text{p}K_a$ in a manner of the discussions above. For example, the additives in drug formulations, such as surfactants, bile salts, phospholipids, ion-pair-forming counterions, cyclodextrins, or polymers may make the drug molecule appear more soluble. As long as such excipients do not undergo a change of charge state in the pH range of interest (i.e., the excipients are effectively non-ionizable), and the drug molecule is ionizable in this range, the difference between the apparent $\text{p}K_a$, $\text{p}K_a^{\text{app}}$, and the true $\text{p}K_a$ will reveal the true aqueous solubility, as if the excipient were not present. Table 6.2 summarizes some of the relationships developed between solubility, $\text{p}K_a$, and $\text{p}K_a^{\text{app}}$.

6.5.5 Results of Aqueous Solubility Determined from Δ Shifts

Since the $\text{p}K_a$ values of the compounds studied are reliably known (Table 6.1), it was possible to calculate the Δ shifts (Table 6.2). These shifts were used to calculate the corrected aqueous intrinsic solubilities S_0 , also listed in Table 6.2.

TABLE 6.2 True Aqueous Solubility Determined from $\text{p}K_a$ Shifts of Monoprotic Compounds

Ionizable Compound Type	$\Delta = \text{p}K_a^{\text{APP}} - \text{p}K_a$	True Aqueous $\log S_0$	Examples
Acid	$\Delta > 0$	$\log S_0^{\text{APP}} - \Delta$	Diclofenac, furosemide, indomethacin, probenecid, naphthoic acid
Acid	$\Delta \leq 0$	$\log S_0^{\text{APP}}$	Prostaglandin F2a [485]
Base	$\Delta \geq 0$	$\log S_0^{\text{APP}}$	Phenazopyridine
Base	$\Delta < 0$	$\log S_0^{\text{APP}} + \Delta$	Amitriptyline, chlorpromazine, miconazole, terfenadine

**Table 6.3 Solubility Constants of Drug Molecules,
Measured by the Dissolution Template
Titration Method^a**

Compound	$-\log S_0$ (log mol L ⁻¹)	Ref.
Acyclovir	2.24	506
Amiloride	3.36	506
Amiodarone	8.10	<i>p</i> ION
Amitriptyline	5.19	506,— ^b
Amoxicilin	2.17	506
Ampicillin	1.69	<i>p</i> ION
Atenolol	1.30	473
Atropine	1.61	506
Benzoic acid	1.59	474
Benzydamine	3.83	472
Bromocriptine	4.70	509
Cephalexin	1.58	<i>p</i> ION
Chlorpromazine	5.27	506,— ^b
Cimetidine	1.43	474
Ciprofloxacin	3.73	506
Clozapine	3.70	509
Desipramine	3.81	506
Diclofenac	5.59	473
Diltiazem	2.95	474
Doxycycline	2.35	506
Enalapril	1.36	474
Erythromycin	3.14	506
Ethinyl estradiol	3.95	506
Famotidine	2.48	473
Flurbiprofen	4.36	473
Furosemide	4.75	473
Hydrochlorothiazide	2.63	473
Ibuprofen	3.62	473
Indomethacin	5.20	506,— ^b
Ketoprofen	3.33	473
Labetolol	3.45	473
Lasinavir	4.00	509
Methotrexate	4.29	506
Metoprolol	1.20	474
Miconazole	5.85	25
Metolazone	4.10	509
Nadolol	1.57	474
Nalidixic acid	4.26	<i>p</i> ION
2-Naphthoic acid	3.93	25
Naproxen	4.21	473
Norfloxacin	2.78	<i>p</i> ION
Nortriptyline	4.18	<i>p</i> ION

Table 6.3 (Continued)

Compound	$-\log S_0$ (log mol L ⁻¹)	Ref.
Phenazopyradine	4.24	506,— ^b
Phenytoin	4.13	473
Pindolol	3.70	<i>p</i> ION
Piroxicam	5.48	<i>p</i> ION
Primaquine	2.77	506
Probenecid	5.68	25
Promethazine	4.39	506
Propoxyphene	5.01	474
Propranolol	3.62	473
Quinine	2.82	474
Rufinamide	3.50	509
Tamoxifen	7.55	506
Terfenadine	6.69	474
Theophylline	1.38	506
Trovafloxacin	4.53	474
Valsartan	4.20	509
Verapamil	4.67	506
Warfarin	4.74	506
Zidovudine	1.16	506

^aTemperature 25°C, 0.15 M ionic strength (KCl).

^bM. A. Strafford, A. Avdeef, P. Artursson, C. A. S. Johansson, K. Luthman, C. R. Brownell, and R. Lyon, Am. Assoc. Pharm. Sci. Ann. Mtng. 2000, poster presentation.

6.6 LIMITS OF DETECTION

The HTS method of Section 6.4.5 can reproduce to 0.1 µg/mL. Turbidity-based methods have sensitivities well above 1 µg/mL. The pH-metric method can decrease to 5 ng/mL [Avdeef, unpublished]. Reports of such a low limit of detection can be found in the literature [495].

6.7 log S_0 "GOLD STANDARD" FOR DRUG MOLECULES

Table 6.3 lists a set of reliably determined log S_0 solubility constants for a series of ionizable drugs determined by the pH-metric DTT solubility method.